STRUCTURE AND DISPERSION OF IRON-BASED DIRECT COAL LIQUEFACTION CATALYSTS

G. P. Huffman, Bhaswati Ganguly, Mehdi Taghiei, F. E. Huggins and Naresh Shah
CFFLS, 233 Mining & Mineral Resources Bldg., University of Kentucky, Lexington, KY 40506-0107

Keywords: liquefaction, catalyst, iron, Mössbauer, XAFS.

Abstract

Mössbauer spectroscopy and X-ray absorption fine structure (XAFS) spectroscopy have been used to characterize the atomic structure and size dispersion of iron-based direct coal liquefaction (DCL) catalysts synthesized by a variety of methods. Samples investigated included a sulfated Fe_2O_3 catalyst, iron added to several coals by chemical impregnation, and iron added to lignite by cation exchange. In the as-dispersed state, all of these catalysts were in the form of superparamagnetic ferric oxides or oxyhydroxides. Size distributions were determined by measuring the percentages of iron contributing to magnetic hyperfine Mössbauer spectra at several temperatures between liquid helium and room temperature, and relating each temperature to a critical particle volume. Size information was also obtained from third and fourth nearest neighbor (nn) iron shell peak amplitudes in radial structure functions derived from the XAFS spectra.

Introduction

There has been much interest in recent years in the use of highly dispersed iron-based DCL catalysts. Several groups have developed methods of preparing such catalysts in very highly dispersed forms.[1-14] It is clearly of interest to develop methods for determining the structure and size of such catalysts. ^{57}Fe Mössbauer spectroscopy has been used by a number of researchers to characterize DCL catalysts.[3,13-20] Yamashita et al.[20] have conducted complementary Mössbauer and XAFS spectroscopy studies on iron-based catalysts in coal.

In the current study, Mössbauer and XAFS spectroscopies have been used to characterize highly dispersed iron-based DCL catalysts prepared by several different research groups. The samples studied included Fe_2O_3 dispersed on carbon black,[21] iron incorporated into coal by chemical impregnation with $FeCl_3$,[5-7] a sulfated Fe_2O_3 catalyst,[9,10] and iron added to lignite by cation exchange.

Experimental Procedure

Catalyst preparation and the efficacy of the various catalysts in DCL have been discussed elsewhere.[1-14] The iron cation-exchanged lignites were prepared in our own laboratory using procedures outlined by Walker and coworkers.[22-24] A lignite from the Penn State sample bank (PSU 1482, Hagel seam) was used.

A standard constant acceleration Mössbauer spectrometer was used. Experimental and least squares analysis procedures are discussed elsewhere.[25,26] Sample temperatures were varied between 12 and 295 K using a Displex cryogenic system.

The XAFS measurements were conducted on beamline X-19A at the National Synchrotron Light Source (NSLS) and beamline IV-1 at the Stanford Synchrotron

Radiation Laboratory (SSRL). X-ray energy was varied using Si(111) double crystal monochromators. All experiments were conducted in the fluorescent mode as described elsewhere.[27]

Results and Discussion

Typical Mössbauer spectra are shown in Figures 1 and 2, which show the spectra obtained at room temperature and 12K from a Wyodak coal impregnated with Fe from an $FeCl_3$ solution[5-7] and from an Fe_2O_3 on carbon black catalyst.[21] All spectra were typical of superparamagnetic ferric oxides. As discussed in more detail elsewhere,[28] the spectra were least squares fitted a series of Lorentzian peaks constrained as quadrupole doublets or magnetic sextets. For most samples, the quadrupole doublet component of the spectrum was dominant at room temperature and exhibited Mössbauer parameters typical of a ferric oxide or oxyhydroxide (isomer shift ≈ 0.34 to 0.39 mm/s, quadrupole splitting ≈ 0.60 to 0.70 mm/s), while the magnetic component became dominant at low temperature and exhibited ferric isomer shifts (0.45 to 0.50 mm/s) and a range of magnetic hyperfine fields (450 to 540 kilogauss). For the samples prepared by Shabtai et al.[5-7] and the cation-exchanged lignites, the Mössbauer parameters were consistent with a superparamagnetic iron oxyhydroxide, while those observed for the Fe_2O_3/SO_4^{-2} and Fe_2O_3 on carbon black were consistent with very fine particle hematite.

As discussed elsewhere,[29-31] when a magnetically ordered particle is small enough, thermal vibrations may cause the ordered spins of the particle to flip over the magnetic anisotropy energy barrier to a new orientation. To a first approximation, the frequency of spin flipping is given by

$$f = f_o \exp\left(\frac{-K_a V}{kT}\right) \tag{1}$$

where K_a is the magnetic anisotropy constant, V is the volume of the particle, k is the Boltzman constant and T is the temperature. The frequency factor f_o is given by Kundig et al.[29] as

$$f = K_a A/\rho N_L h \tag{2}$$

where A is the molecular weight, ρ is the density, N_L is Avogadro's number, and h is the Planck constant. For the magnetic anisotropy constants, we have used the values give by van der Kraan;[31] $K_a = 0.55 \times 10^5$ joule/m^3 for hematite, and $K_a = 1.67 \times 10^5$ joule/m^3 for goethite. Eq. (2) then gives $f_o = 4.2 \times 10^9$ sec^{-1} for hematite and $f_o = 8.7 \times 10^9$ sec^{-1} for goethite. When f is small compared to the nuclear Larmor precession frequency of the ^{57}Fe nuclear magnetic moment ($f_L = 5 \times 10^7$ sec^{-1}), the particle will exhibit a well-resolved six line magnetic hyperfine spectrum. However, when f becomes comparable to or exceeds f_L, the magnetic spectrum collapses to a two peak quadrupole doublet. Putting f equal to f_L and rewriting Eq. (1), we obtain

$$V_c = \frac{kT}{K_a} \ln\left(\frac{f_o}{f_L}\right) \tag{3}$$

Eq. (3) can be viewed as defining a critical volume, V_c, for temperature T. At temperature T, to a first approximation, particles of volume > V_c will give rise to a six-line magnetic hyperfine spectrum, while particles of volume < V_c will exhibit a

paramagnetic quadrupole doublet.

The temperature variation of the magnetic and paramagnetic (quadrupole) percentages is then used with Eq. 3 to generate size distributions. The results are summarized in Figure 3 for all of the as synthesized catalysts investigated by size histograms that show the percentage of iron contained in ferric oxide particles as a function of particle diameter. Spherical particles are assumed in order to derive diameters from the volumes given by Equ. (3). The resolution of these size distributions depends, of course, on the number of temperatures at which spectra are obtained. As discussed in more detail elsewwhere, [28] the error in the diameters indicated in these histograms is approximately ± 5 - 10 Å, while the error in the iron percentages is about ± 5%.

It is seen that most of the catalyst particles in all of the catalysts examined are smaller than approximately 65 - 85 Å in diameter, with from 10 to 70% of the iron contained in particles less than 20-30 Å in diameter. Moreover, many of the particles in the smallest size bin may be of molecular dimensions. It is also seen that the samples prepared by the Shabtai $FeCl_3$ impregnation method[5-7] exhibit the smallest size distributions. During the mild hydrotreatment (290°C, 1500 psig H_2 hot, 2 hours) used by Shabtai and coworkers,[5-7] the iron remains in the form of a ferric oxide or oxyhydroxide and the particle sizes increase somewhat, as seen in Figure 5.

Fourier transformation of the extended X-ray absorption fine structure (EXAFS) of the XAFS spectrum produces a radial structure function (RSF) that is similar to a radial distribution function. Some typical RSFs from the current samples are shown in Figures 4-5. As discussed in detail elsewhere,[32] each peak represents a shell of atoms surrounding the central iron atom. The peak positions on the distance axis are shifted slightly downward by about 0.5 Å relative to the true interatomic distances because of phase shifts, and the peak amplitudes are proportional to several factors, one of which is the shell coordination number.

In Figure 5, the radial structure function (RSF) of α-Fe_2O_3 is compared to that of the Fe_2O_3/SO_4^{-2} catalyst. It is seen that the amplitudes of the peaks arising from the third and fourth nearest neighbor (nn) iron shells in the catalyst are significantly reduced relative to those of the same shells in bulk α-Fe_2O_3. For the cation-exchanged samples and for all of the Shabtai samples, before and after hydrotreatment, the RSFs are similar to that of goethite, but in most cases the third and fourth nn Fe shells are nearly undetectable. This is illustrated by Figure 4.

One explanation of the decreased amplitudes of the third and fourth nn iron shell peaks is that the iron atoms at or near the surfaces of these very small catalyst particles do not have their full complement of third and fourth iron nn. Since it may reasonably be expected that the first nn oxygen coordination of these iron atoms is unchanged, a convenient measure of the decrease in the average number of iron atoms in the third and fourth nn shells is the ratio of those peak heights in the RSF to that of the oxygen first nn shell. These peak height ratios are summarized for all catalyst samples and for the appropriate standard compounds in Table 1. Assuming that these ratios are proportional to the ratios of the coordination numbers, we can deduce the average iron coordination numbers for the catalysts by comparing their peak height ratios to those of the standard compounds for which the coordination numbers are known. These results are also indicated in Table 1. It is of interest to note that the third and fourth nn shell peaks are essentially absent from the RSFs of several of the Shabtai and cation-exchanged samples. However, because of the noise level of the RSFs, the lowest peak height ratio that can be reliably determined from the current data is approximately 0.2. Therefore, we can only put a lower limit on coordination numbers for these samples.

Table 1. Summary of peak height information from RSFs. H/H_{OX} is the ratio of the height of the peak from the iron shell to that of the oxygen nn shell.

Sample	Peak No.	Shell type	Distance (Å)	H/H_{OX} (±0.1)	Coord. No. (±1)
Magnetite, Fe_3O_4	3	Fe	2.97	1.65	8
	4	Fe	3.49	1.69	12
PSOC 1482, ion ex.	3	Fe		1.00	4.8
0.5M $Fe(OOCCH_3)_2$	4	Fe		1.07	7.6
Hematite, 2-Fe_2O_3	3	Fe	2.88, 2.97 <2.95>	1.74	1, 3 } 4
	4	Fe*	3.70	1.27	6
Fe_2O_3/SO_4^{-2}	3	Fe		0.91	2.1
	4	Fe*		0.70	3.3
Fe_2O_3 on carbon black	3	Fe		1.03	2.4
	4	Fe*		0.58	2.7
Goethite, α-FeOOH	3	Fe	3.01, 3.21, 3.42 <3.28>	0.80	2, 2, 4 } 8
PSOC 1482, ion ex., 0.02 M Fe $(OOCCH_3)_2$	3	Fe		0.43	4.3
PSOC 1482, ion ex., $FeCL_2$	3	Fe		<0.2	<2
Blind Canyon [$FeCl_3$ treated - Shabtai]	3	Fe		<0.2	<2

*Oxygen neighbor shells also contribute to this peak.

Summary and Conclusions

A variety of iron-based liquefaction catalysts have been investigated by Mössbauer and XAFS spectroscopy. Samples investigated included coals subjected to an $FeCl_3$ impregnation treatment described by Shabtai and coworkers,[5-7] a highly dispersed Fe_2O_3 on carbon black catalyst,[21] iron dispersed in a lignite by cation exchange, and a sulfated hematite catalyst (Fe_2O_3/SO_4^{-2}) prepared by Wender and coworkers,[9,10]. The results may be summarized briefly as follows:

1. Both Mössbauer and XAFS spectroscopies can determine the structure of the catalysts and provide information on their size. The Mössbauer technique is more accurate but is also a much slower measurement, typically requiring 10-20 hours, while the XAFS measurement normally requires about 30-60 minutes.
2. In all cases, the initial as-dispersed or as-prepared catalyst is in the form of a highly dispersed ferric oxide or oxyhydroxide.
3. Because of superparamagnetic relaxation effects, the Mössbauer spectra exhibit a

significant increase in the percentage of iron contributing to magnetic hyperfine patterns as the sample temperature is lowered. These magnetic hyperfine percentages may be converted into particle size distributions which indicate that the size of the as-dispersed ferric oxyhydroxides and oxides range from molecular to particles ~20 - 100 Å in diameter.

A more detailed discussion of these results will be given elsewhere.[28]

Acknowledgement

This research was sponsored by the U.S. Department of Energy under DOE Contract No. DE-FC22-90PC90029. The NSLS and SSRL facilities are also sponsored by the U.S. DOE. We are grateful to Dr. Joseph Shabtai of the University of Utah, Dr. Irving Wender of the University of Pittsburgh and Dr. Malvina Farcasiu of the U.S. DOE Pittsburgh Energy Technology Center for providing us with samples.

References

1. Suzuki, T.; Yamada, O.; Takehaski, Y.; Watanabe, Y. *Fuel Process. Technol.*, **1985**, *10*, 33-43.
2. Watanabe, Y.; Yamada, O.; Fujita, K.; Takegami, Y.; Suzuki, T. *Fuel* **1984**, *63*, 752-755.
3. Herrick, D. E.; Tierney, J. W.; Wender, I.; Huffman, G. P.; and Huggins, *Energy and Fuels*, 1990, *4*, 231-236.
4. Herrick, D. E., Ph.D. Thesis, University of Pittsburgh, **1990**.
5. Shabtai, J. S.; Saito, I.; U.S. Patent, 4,728,418 (1988).
6. Shabtai, J. S.; Zhang, Y. *Proc. 1989 Internat. Confer. Coal Science*, Tokyo **1989**, Vol. II, 807-810.
7. Shabtai, J. S., Skulthai, T. *Proc. 1987 Internat. Conference Coal Science* Maastricht, The Netherlands, Elsevier, 761-764.
8. Marriadassou, D. G.; Charcosset, H.; Andres, M; Chiche, P.; *Fuel*, **1986**, Vol. 62, pp. 69-72.
9. Pradhan, V. R. ; Tierney, J. W.; Wender, I.;' Preprints, Div. of Fuel Chem., *American Chemical Society*, August **1990**, vol. 35, No. 3, p. 793.
10. Pradhan, V. R.; Tierney, J. W.; Wender, I.; and Huffman, G. P.; **1991**, submitted to *Energy & Fuels*.
11. Tanabe, K.; Yamaguchi, T.; Hattori, H.; Sanada, Y.; Yuokoyama, S.; *Fuel Processing Technology*, **1984**, Vol. 14, pp. 247-260.
12. Tanabe, K.; Tamaguchi, T.; Hattori, H.; Matsuhashi, H.; Kimura, A.; *Fuel Processing Technology*, **1986**, Vol. 8, pp. 117-122.
13. Cook, P. S. and Cashion, J. D.; *Fuel*, **1987**, *66*, 661-668.
14. Cook, P. S. and Cashion, J. D.; *Fuel*, **1987**, *66*, 669-677.
15. Montano, P. A. and Granoff, F., *Fuel*, **1980**, *59*, 214.
16. Montano, P. A.; Bommannavar, A. S.; and Shah, V.; *Fuel*, **1981**, *60*, 703.
17. Bommannavar, A. S. and Montano, P. A.; *Fuel*, **1982**, *61*, 523.
18. Ogawa, T.; Stenberg, V. I.; and Montano, P. A.; *Fuel*, **1984**, *63*, 1660-1663.
19. Montano, P. A.; Stenberg, V. I.; and Sweeny, P.; *J. Phys. Chem.*, **1986**, *90*, 156-159.
20. Yamashita, H.; Oktsuka, Y.; Yoshida, S.; and Tomita, A.; *Energy & Fuels*, **1989**, *3*, 686.
21. Sample provided by Malvina Farcasiu, U. S. DOE Pittsburgh Energy Technology Center.
22. Walker, Jr., P. S.; Matsumoto, S.; Hanzawa, T.; Murira, T.; Ismail, I. M. K.; *Fuel*, **1983**, *62*, 140-149.
23. Jenkins, R. G.; Nandi, S. P.; and Walker, P. L.; *Fuel*, **1973**, *52*, 288.

24. Mahajan, O. P.; Yarzab, R; and Walker, P. L.; *Fuel*, **1978**, *57*, 643.
25. Huffman, G. P.; Huggins, F. E.; *Fuel* **1978**, *47*, 592-604.
26. Huggins, F. E.; Huffman, G. P. Mössbauer Analysis of the Iron-Bearing Phases in Coal, Coke, and Ash. *Analytical Methods for Coal and Coal Products*; Karr, Jr., C., Ed.; Academic Press: New York, 1979; Vol. III p. 371-423.
27. Lytle, F. W.; Greegor, R. B.; Sandstrom, D. R.; Marques, E. C.; Wong, Joe; Sprio, C. L.; Huffman, G. P.; and Huggins, F. E.; *Nucl. Instrum & Methods*, **1984**, *226*, 542-548.
28. Huffman, G. P.; Huggins, F. E.; Ganguly, B.; Taghiei, M.; and Shah, N., "Structure and Dispersion of Iron-Based DCL Catalysts," submitted to *Energy & Fuels*.
29. Kundig, W.; Bömmel, Constabaris, G.; Lindquist, R. H.; *Phys. Rev.*, **1966**, *142*, 327.
30. Wickman, H. H.; "Mössbauer Paramagnetic Hyperfine Structure," pp. 39-66, *Mössbauer Effect Methodology*, Ed. I. J. Gruverman, Plenum Press, NY, 1966.
31. van der Kraan, A. M.; *Phys. Stat. Sol.* **1973**, (a) *18*, 215.
32. Lee, P. A.; Citrin, P. H.; Eisenberger,; and Kincaid, B. M.; *Rev. Mod. Phys.*, **1981**, *53*, 769-806.

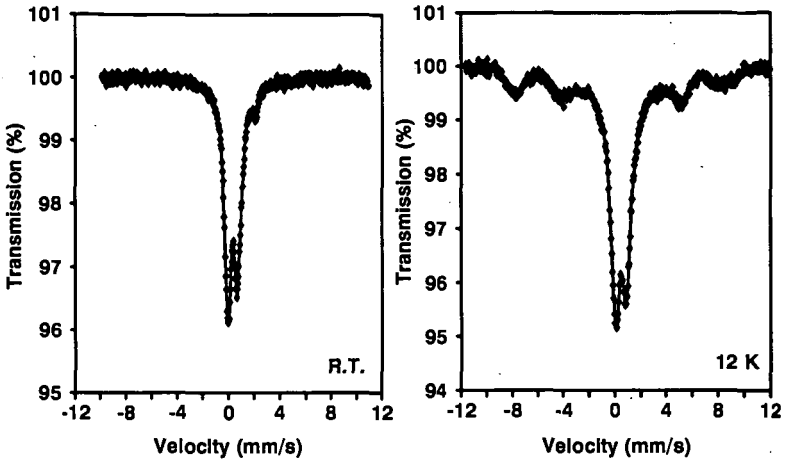

Figure 1- Room temperature and 12 K Mössbauer spectra of a Wyodak coal impregnated with iron by the Shabtai treatment.

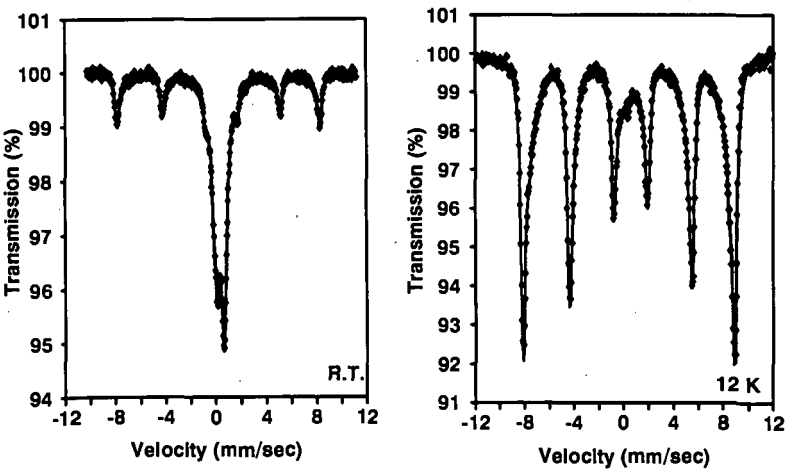

Figure 2- Room temperature and 12K Mössbauer spectra of an Fe2O3 on carbon black catalyst.

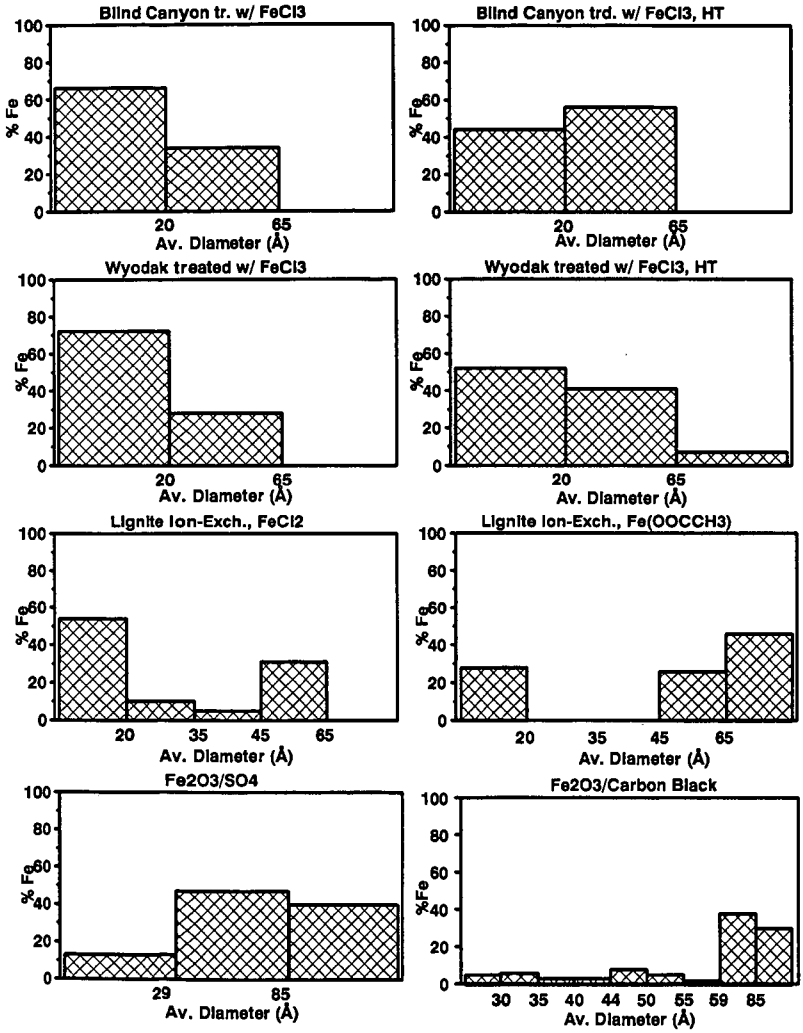

Figure 3- Size distribution for various as-dispersed iron DCL catalysts derived from Mössbauer data.

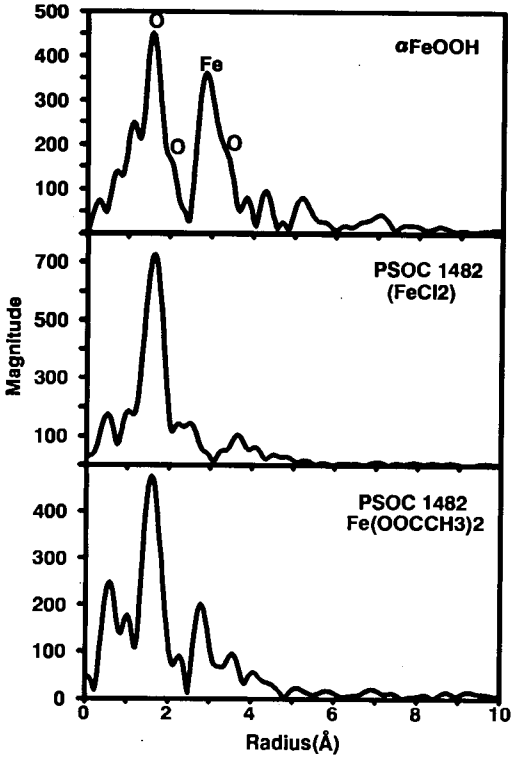

Figure 4. RSF's of goethite and two iron cation-exchanged lignites.

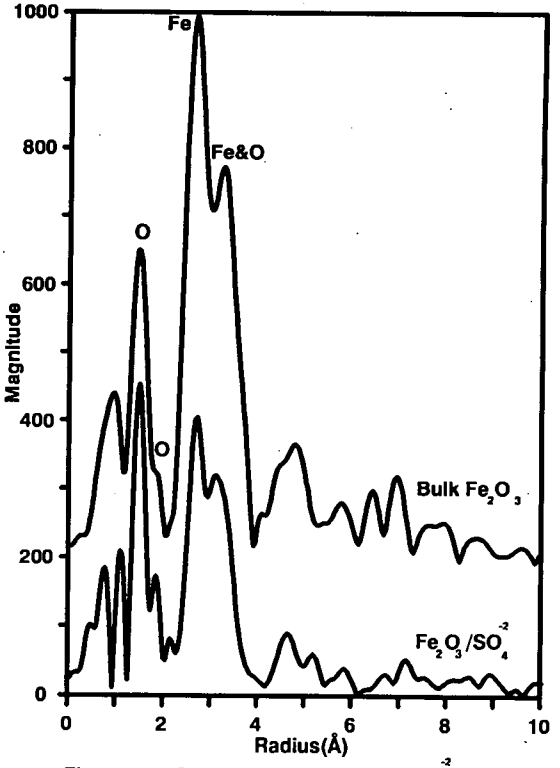

Figure 5. RSF's of hematite and Fe_2O_3/SO_4^{-2} catalyst.